PNAS

Supporting Information for

Diverse cytomegalovirus US11 antagonism and MHC-A evasion strategies reveal a tit-for-tat coevolutionary arms race in hominids

Cosima Zimmermann¶, Gabrielle M. Watson¶, Liane Bauersfeld, Richard Berry, Barbara Ciblis, Huan Lan, Carolin Gerke, Valerie Oberhardt, Jonas Fuchs, Maike Hofmann, Christian Freund, Jamie Rossjohn, Frank Momburg, Hartmut Hengel, Anne Halenius

¶These authors contributed equally to this work

Corresponding author: Anne Halenius
Email: anne.halenius@uniklinik-freiburg.de

This PDF file includes:

Materials and Methods

Molecular cloning

N-terminally HA-tagged HLA-I molecules and chimeras were cloned into the Tpn-SP-HA-pIRES-EGFP vector via PstI or NsiI and BamHI as previously described [1]. Either specific primers were used for amplification or a synthetic DNA was used. The HA-HLA-I cDNA was subcloned (NheI and BamHI.) into the puc2CL6IP vector (SFFV U3 promoter) that was used for transient expression of HLA-I molecules. HA-HLA-A*02:01 and B*07:02 chimeras were constructed by combining nucleotides encoding the first 181 amino acids with the direct downstream sequence of the other HLA-I molecule. HA-HLA-A*02:01 and A*03:01 chimeras were constructed by swapping the PstI fragments. For mutation of single residues, the Q5 site-directed mutagenesis kit (New England Bio Labs) was applied. The HLA-A*02:01 disulfide-trapped single-chain trimer loaded with the HCMV $pp65_{495-503}$ peptide NLVPMVATV (SC_{NLV}) was cloned as described previously [2], incorporating a full-length HLA-A*02:01 cDNA with mutation Y84C at the 3' end of the second glycine-serine linker sequence. In the disulfide-stabilized HLA-A*02:01 single-chain dimer (SC_{DS}), the peptide sequence and first glycine-serine linker sequence was deleted putting the human β_2-microglobulin ORF directly after the influenza haemagglutinin ER leader sequence. In addition to Y84C, the mutation A139C was introduced into the HLA-A*02:01 sequence by PCR-directed mutagenesis. The US11-SC constructs were designed on the basis of the SC_{DS} construct. The haemagglutinin ER leader sequence and the following linker sequence were replaced by the US11 sequence (encoding amino acids 1-43) and a shorter linker (GSGGGGAPGSGGGSLGS). In addition, mutated amino acids in the HLA-A*02:01 sequence were corrected (to Tyr84 and Ala139). US11-SC, $US11_{L25G}$-SC, SC-A29, and US11-SC-A29 were synthesized and cloned into pcDNA3.1 by BioCat (Heidelberg). For construction of HLA-A*02:01 SC the amino acids positions 84 and 139 in SC_{DS} was corrected to Tyr and Ala, respectively.

The cUS11 (panine herpesvirus 2 strain Heberling, NC_003521.1), chimeric US11 sequences and ligand-US11 variants were obtained as gBlocks and cloned into pIRES-EGFP via NheI and BamHI. In h/cUS11 the sequence encoding the first 44 amino acids of hUS11 was fused to the sequence encoding the region 55-225 of cUS11. In the c/hUS11 chimera the sequence encoding amino acids 21-44 in hUS11 was exchanged to the sequence encoding amino acids 18-54 in cUS11. In the HLA-A ligand-US11 constructs, a signal peptide sequence from the influenza haemagglutinin protein (MAKANLLVLLCALAAADA) was placed in front of the peptide ligand sequence. Between the peptide and the US11 sequence (amino acids 43-215) a 21 amino acid long linker ($GGSLS(GGGS)_2ASGGGG$) was inserted. The following peptide sequences were used: HLA-A*02:01: pp65-NLV (NLVPMVATV); HLA-A*29:02: US27-LYV (LYVGQFLAY); HLA-A*68:02: EVI (EVIDFSHGL); HLA-A*03:01: UL77-GLY (GLYTQPRWK). All peptides were previously detected in

MHC-I ligandome analyses [1, 3]. For MHC-I peptide binding predictions we applied NetMHCpan 4.1 [4].

Viruses

To generate the HCMV mutant viruses +US11 and +Δ_NUS11 the corresponding sequences were cloned into the vector pGPS-Kn-rox [5]. The US11 sequence and the kanamycin cassette were amplified for BAC2 (AD169VarL BAC [6, 7] recombination using the following primers: LB-US11_Kana1, TTACAGCTTTTGAGTCTAGACAGGGTAACAGCCTTCCCTTGTAAGACAGAATGAACCTTGTAATGCTTATTCTA and LB-US11_Kana2, GGTGAGTCGTTTCCGAGCGACTCGAGATGCACTCCGCTTCAGTCTATATATGTGGGCGGACAAAATAGTTGG.

Antibodies and reagents

The following mAbs were used: HC10, which binds free HCs [8], anti-HLA-A*02:01 (BB7.2) [9], and anti-β_2m (BBM.1) [10]. Mouse anti-HA, mouse anti-β-actin, HRP-coupled goat anti-rabbit IgG, PMA, ionomycin, accutase, cysteine and methionine were purchased from Sigma-Aldrich, and APC-coupled anti-HA, FITC-coupled anti-HLA-A*02:01 (REA517), APC-coupled anti-HLA-A*03 (REA950), IgG isotype controls and FcR blocking reagent from Miltenyi Biotec. We used APC-coupled goat anti-mouse IgG, FITC-coupled anti-IFNγ, anti-CD28 antibody and PE-conjugated anti-CD8 from BD Biosciences, and PE/Cy7-coupled anti-TNFα and IFNγ from BioLegend. Further, we used HRP-coupled goat anti-mouse IgG (Dianova), viability dye eFluors™ 506 (Ebioscience), IL-2 (Stemcell), SignalFire ECL Reagent (Cell Signaling Technology), streptavidin-R-PE (Agilent), Easytag Express ^{35}S-Met-Cys protein labeling mix (Perkin Elmer), protein A Sepharose (GE Healthcare), and Digitonin (Calbiochem). Anti-US11 has been described [1].

Protein expression and purification

A single chain construct ($_{US11}$SC) encoding the US11 N-terminus (residues 17-43), a 17 amino acid Gly-Ser rich linker, β_2m (residues 21-119), a 27 amino acid Gly-Ser rich linker, and HLA-A*02:01 (residues 25-298), was codon optimised for expression in *E. coli* (Integrated DNA technologies) and cloned into the pET30 expression vector. $_{US11}$SC was expressed as inclusion bodies in Ton A-BL21 (DE3) *E. coli*, solubilised in 6 M guanidine-HCl and subsequently refolded by rapid dilution in a buffer comprising 100 mM Tris pH 8.0, 400 mM L-arginine, 3 M urea, 2 mM EDTA, 0.2 mM phenylmethyl sulfonyl fluoride (PMSF), 0.5:5 mM oxidised:reduced glutathione for 3 d at 4°C. Following dialysis into 10 mM Tris pH 8.0, refolded $_{US11}$SC was purified by a combination of anion exchange (DEAE and Hitrap Q, Cytiva) and size exclusion (Superdex 200, Cytiva) chromatography systems. Following size exclusion chromatography in a buffer comprising 10 mM Tris pH 8.0, 150

mM NaCl, purified $_{US11}$SC was concentrated to 5.2 mg/mL for crystallisation4 experiments. Isolated β_2m and the HLA-A*02:01 were also expressed as inclusion bodies in Ton A- BL21 (DE3) *E. coli*, before being refolded with the TLFDEPPPL peptide in the ratio 3.2 µM HC, 2.6 µM β2m and 11 µM peptide, and purified as described above.

Crystallization

All crystals formed at 20° C via the hanging drop vapour diffusion crystallisation method and microseeded with HLA-A*02:01 crystals obtained from a solution containing 3% (w/v) PEG3350, 0.1 M HEPES pH 7.4, 0.1 M NaCl, 5 mM MgCl2 and 5 mM CdCl2. $_{US11}$SC crystals formed with a reservoir solution containing 30% (*w/v*) PEG3350 and 0.1 M D_L-malic acid pH 7.0. HLA-A*02^{TLF} crystals formed with a reservoir solution containing 26% (*w/v*) PEG3350 and 0.1 M D_L-malic acid pH 7.0. Both crystallisation conditions were supplemented with 83 mM cesium chloride (Hampton Research Additive Screen). Crystals were cryoprotected in mother liquor supplemented with 15-20% (*v/v*) glycerol and flash-cooled in liquid nitrogen.

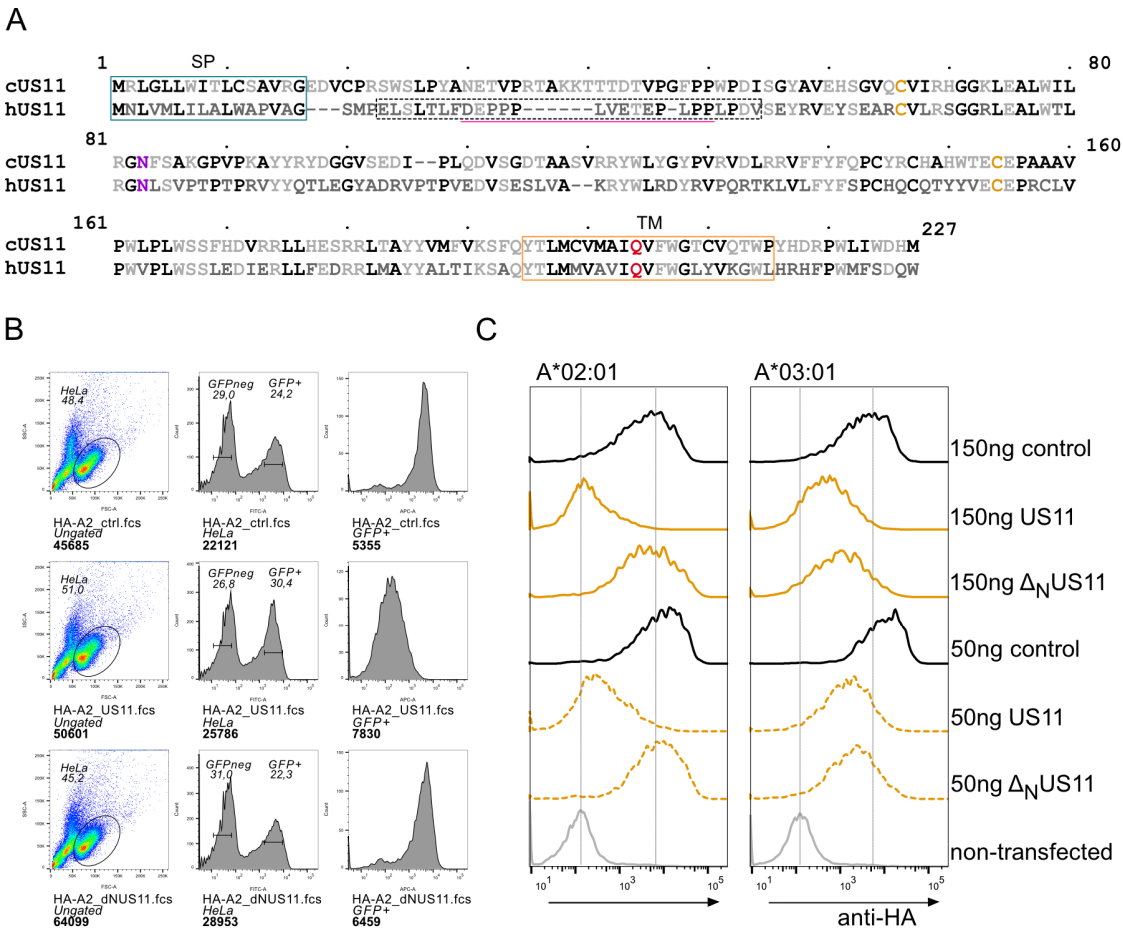

Fig S1. The HCMV encoded immunoevasin US11 differentially regulates surface expression of HLA-A allotypes. (A) Alignment of HCMV and CCMV US11, hUS11 and cUS11, respectively. The predicted signal peptides (SP; SignalP 6.0) and transmembrane domains (TM) are marked by blue and orange boxes, respectively. The orange C's are predicted to form a disulfide bridge in the Ig-like fold [11], the violet N is glycosylated, and the red Q marks the residue that is decisive for Derlin-1 interaction. The pink line shows the HCMV US11 LCR region, lacking in the CCMV US11 (analyzed with PlaToLoCo [12]). The black box with a dashed line marks the N-terminal region that was deleted in Δ_NUS11 (residues 20-44). (B) Example of gates used for determination of HLA-A expression after transient transfection of HeLa cells (Fig 1B). HA-HLA-A*02:01 (HA-A2) is shown with control (ctrl), US11, or Δ_NUS11 (dNUS11). The gates and percent cells in each gate are written in latin. Cell numbers are written in bold. (C) HA-tagged HLA-I expression plasmids were transiently transfected in HeLa cells (ca. $2x10^5$ cells) with 150 or 50 ng of pIRES-EGFP encoding US11, Δ_NUS11 or a control protein. At 20 h post-transfection HLA-I surface expression was determined

by flow cytometry (anti-HA) on EGFP-positive cells. Representative histograms are shown. Vertical lines were included for better comparison of peaks.

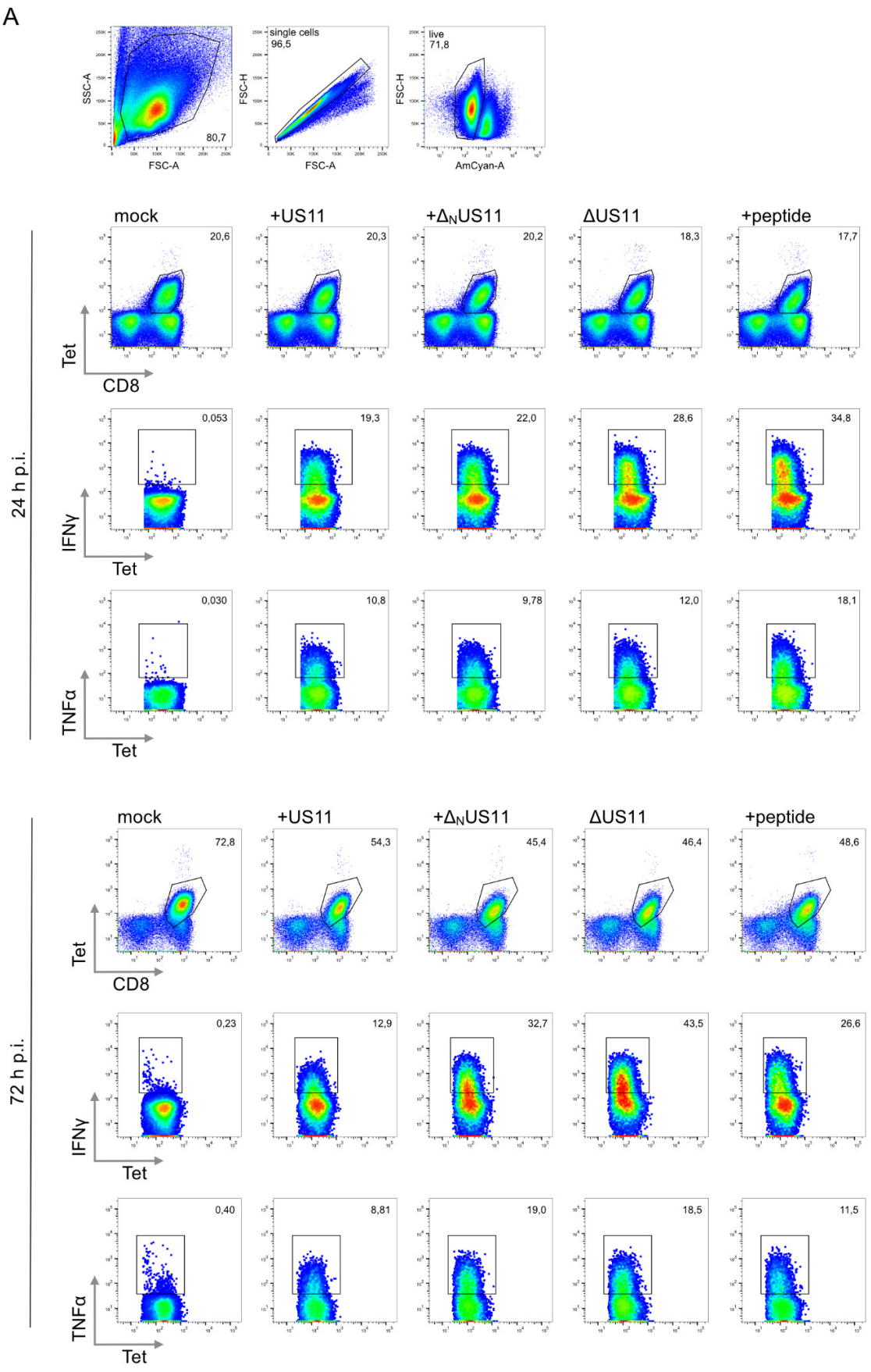
A
SSC-A
FSC-A
80,7
single cells
96,5
FSC-H
FSC-A
live
71,8
FSC-H
AmCyan-A
mock
+US11
+ΔNUS11
ΔUS11
+peptide
24 h p.i.
20,6
20,3
20,2
18,3
17,7
Tet
CD8
0,053
19,3
22,0
28,6
34,8
IFNγ
Tet
0,030
10,8
9,78
12,0
18,1
TNFα
Tet
72 h p.i.
mock
+US11
+ΔNUS11
ΔUS11
+peptide
72,8
54,3
45,4
46,4
48,6
Tet
CD8
0,23
12,9
32,7
43,5
26,6
IFNγ
Tet
0,40
8,81
19,0
18,5
11,5
TNFα
Tet

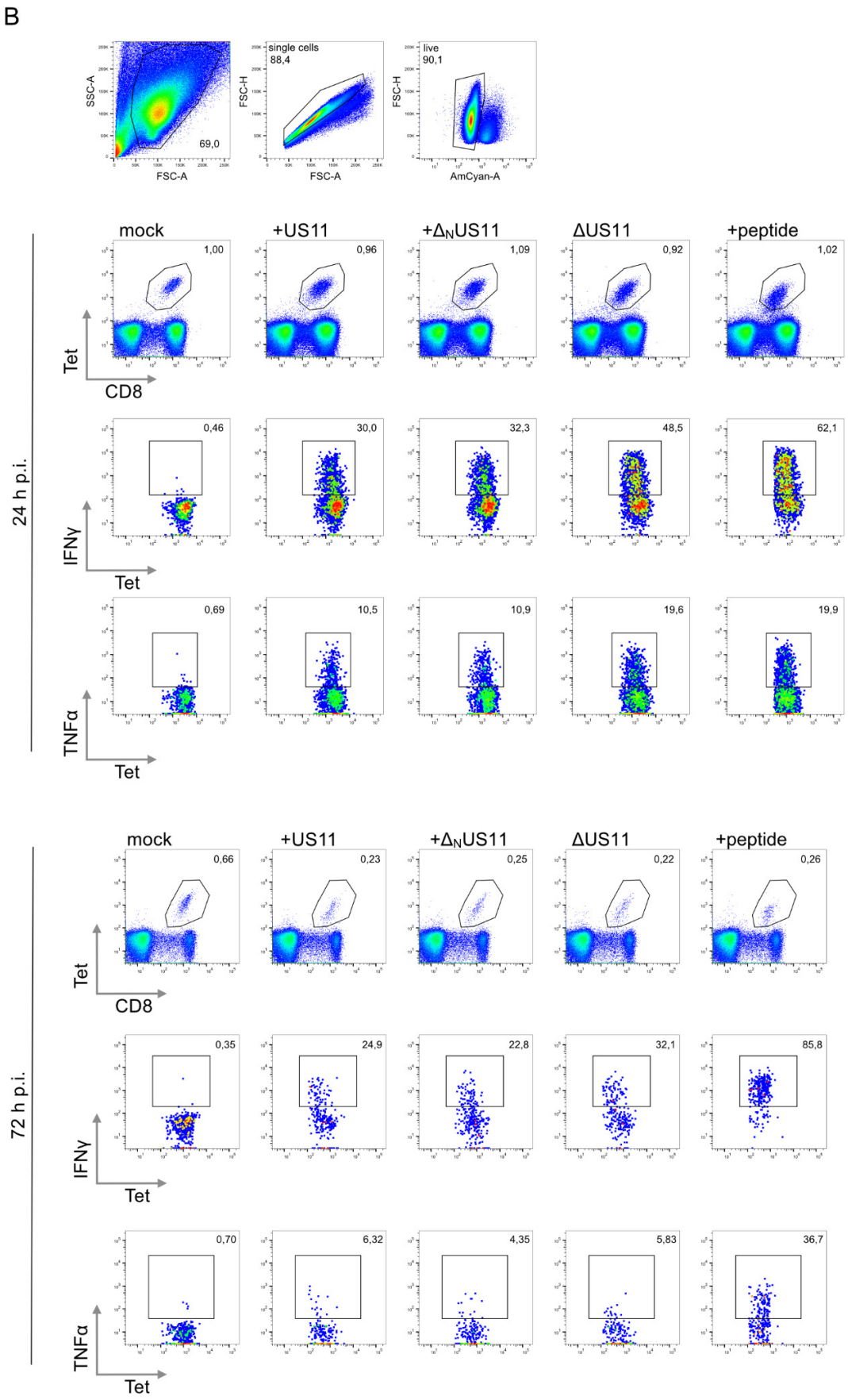
B
SSC-A
FSC-A
69,0
single cells
88,4
FSC-H
FSC-A
live
90,1
FSC-H
AmCyan-A
24 h p.i.
mock
+US11
+ΔNUS11
ΔUS11
+peptide
1,00
0,96
1,09
0,92
1,02
Tet
CD8
0,46
30,0
32,3
48,5
62,1
IFNγ
Tet
0,69
10,5
10,9
19,6
19,9
TNFα
Tet
72 h p.i.
mock
+US11
+ΔNUS11
ΔUS11
+peptide
0,66
0,23
0,25
0,22
0,26
Tet
CD8
0,35
24,9
22,8
32,1
85,8
IFNγ
Tet
0,70
6,32
4,35
5,83
36,7
TNFα
Tet

C % activated CD8+/tetramer+ T cells

		24 h.p.i.				72 h.p.i.			
		Rep 1		Rep 2		Rep 1		Rep 2	
		IFN	*TNF*	*IFN*	*TNF*	*IFN*	*TNF*	*IFN*	*TNF*
HLA-A*02-pp65	US11	42.8	27.1	19.3	10.8	11.4	12.2	12.9	8.8
	ΔN	40.8	22.6	22.0	9.8	22.6	18.7	32.7	19.0
	ΔUS11	41.6	22.8	28.6	12.0	26.0	15.6	43.5	18.5
HLA-A*03-UL77	US11	30.0	10.5	23.6	5.7	26.6	5.0	24.9	6.3
	ΔN	32.3	10.9	19.1	3.7	24.5	4.1	22.8	4.4
	ΔUS11	48.5	19.6	38.9	8.8	26.5	3.7	32.1	5.8

D Fold activated CD8+/tetramer+ T cells (relative to ΔUS11)

		24 h.p.i.				72 h.p.i.			
		Rep 1		Rep 2		Rep 1		Rep 2	
		IFN	*TNF*	*IFN*	*TNF*	*IFN*	*TNF*	*IFN*	*TNF*
HLA-A*02-pp65	US11	1.03	1.19	0.67	0.90	0.44	0.78	0.30	0.48
	ΔN	0.98	0.99	0.77	0.82	0.87	1.20	0.75	1.03
HLA-A*03-UL77	US11	0.62	0.54	0.61	0.64	1.00	1.37	0.78	1.08
	ΔN	0.67	0.56	0.49	0.42	0.92	1.12	0.71	0.75

Fig S2. The US11 LCR protects HCMV from HLA-A*02:01 restricted CD8+ T-cells. (A-B) Example of gating strategy of flow cytometry analysis of intracellular IFNγ and TNFα expression by CD8 T cells in the experiments shown in Fig 2C. HLA-A*02:01^{NLV} and HLA-A*03:01^{GLY} specific polyclonal CD8+ T cells are depicted in panel A and B, respectively. (C) The percentage of activated CD8+/tetramer+ T cells measured in the experiments presented in Fig 2C. (D) Relative values from (C), used in Fig 2C. At 24 h p.i. replicates (Rep1 and Rep2) were performed separately with PBMCs isolated from the same donor at different occasions. At 72 h p.i. replicates were performed in parallel with PBMCs isolated from two different donors.

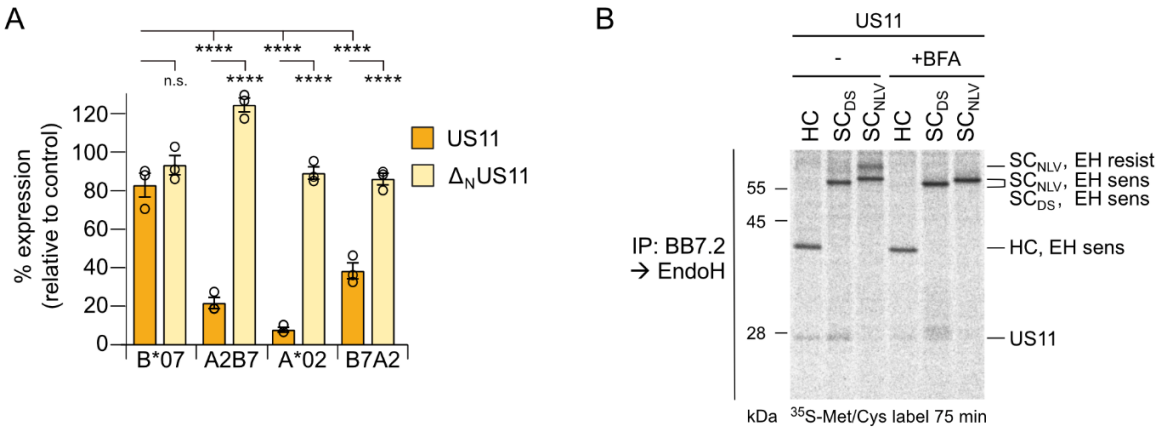

Fig S3. Peptide loaded HLA-A*02:01 confers resistance to US11. (A) The percentage of MFI as compared to control transfected cells was determined from the analysis depicted in Fig 3B. Dots represent individual values and bars mean values ± SEM from three independent experiments. Significance was calculated using two-way ANOVA. (B) HLA-A*02:01 HC or SC constructs encoded in pcDNA3.1 were transiently co-transfected with pIRES-EGFP encoding US11 into HeLa cells. At 20 h post-transfection cells were metabolically labeled for 75 min in the presence or absence of 5µg/mL brefeldin A (BFA). The mAb BB7.2 (anti-HLA-A*02) was applied for immunoprecipitation. Retrieved proteins were EndoH digested as indicated prior to separation on SDS-PAGE and detection by autoradiography.

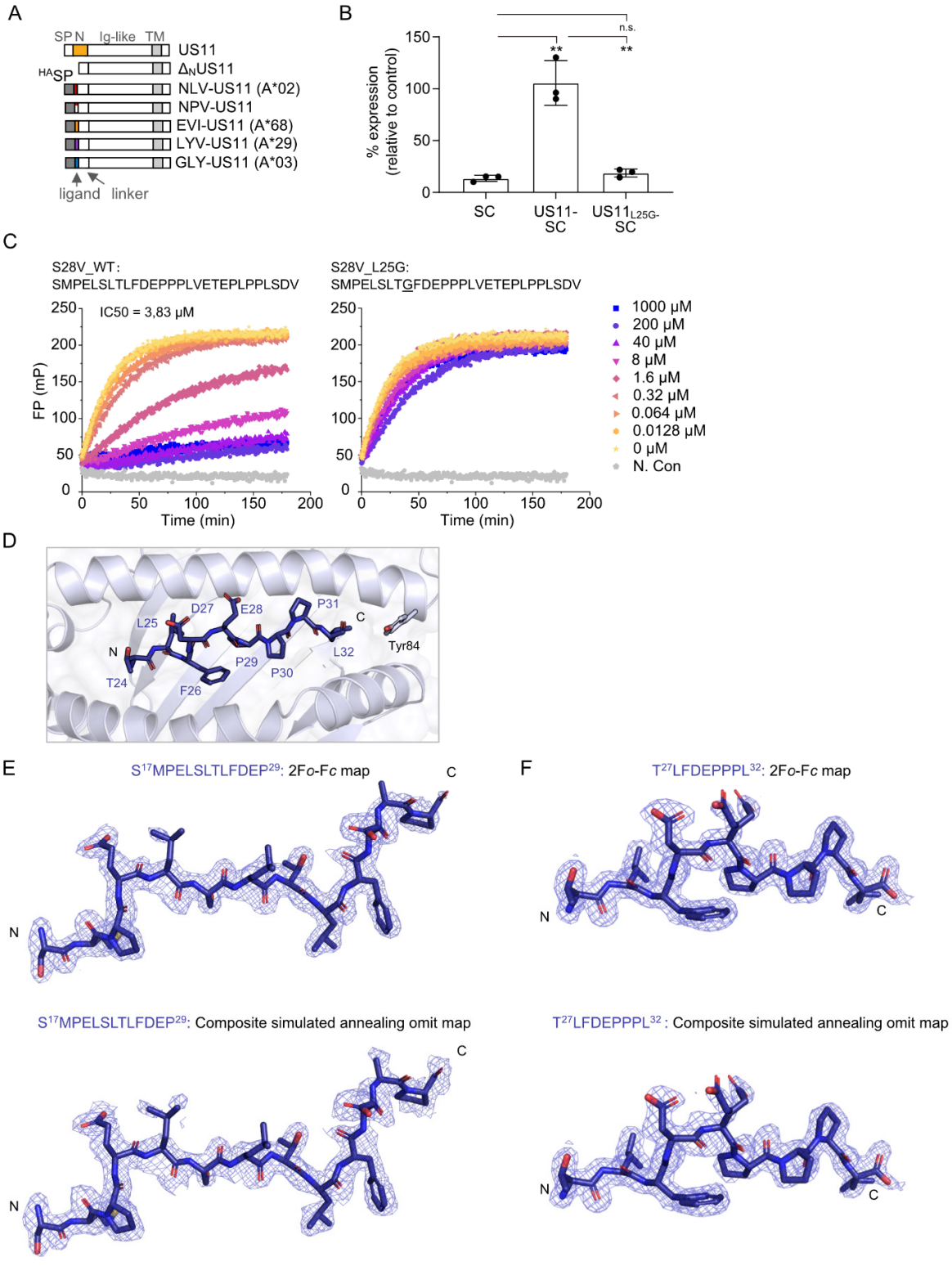
A
SP N Ig-like TM
US11
HASP ΔNUS11
NLV-US11 (A*02)
NPV-US11
EVI-US11 (A*68)
LYV-US11 (A*29)
GLY-US11 (A*03)
ligand linker
B
% expression (relative to control)
n.s.
**
**
SC
US11-SC
US11L25G-SC
C
S28V_WT:
SMPELSLTLFDEPPPLVETEPLPPLSDV
S28V_L25G:
SMPELSLTGFDEPPPLVETEPLPPLSDV
IC50 = 3,83 µM
FP (mP)
Time (min)
1000 µM
200 µM
40 µM
8 µM
1.6 µM
0.32 µM
0.064 µM
0.0128 µM
0 µM
N. Con
D
D27
E28
P31
L25
C
N
L32
Tyr84
P29
P30
T24
F26
E
S17MPELSLTLFDEP29: 2Fo-Fc map
C
N
F
T27LFDEPPPL32: 2Fo-Fc map
N
C
S17MPELSLTLFDEP29: Composite simulated annealing omit map
C
N
T27LFDEPPPL32 : Composite simulated annealing omit map
N
C

Fig S4. The US11 LCR mimics peptide binding to HLA-A*02:01. (A) Schematic representation of chimeric HLA-A ligand-US11 constructs expressed for flow cytometry analysis in Fig 4B-C. (B) The percentage of HLA-A*02:01 SC surface disposition (MFI) in US6 expressing cells as compared to control cells was determined from the analysis depicted in Fig 4F. Dots represent individual values and bars mean values ± SEM from three independent experiments. Significance was calculated using two-way ANOVA. (C) Effect of the US11 peptide (amino acids 17-44; S28V_WT) or a peptide mutated at position 25 (S28V_L25G) on binding of the FITC-labeled peptide GV9 (GILGK^{FITC}VFTV) to HLA-A*02:01 in an MHC-I fluorescence polarization assay. Representative measurements are shown. (D) X-ray crystal structure of HLA-A*02:01 refolded with the US11 LCR derived 9mer peptide T^{27}LFDEPPPL^{32}. HLA-A*02:01 and the peptide are coloured and labelled as in Fig 4H-I (PDB ID: 8FU4). (E-F) Refined $2F_o$-F_c map (top) and composite simulated annealing omit map (bottom) for (E) observed LCR residues (S^{17}MPELSLTLFDEP^{29}) in the US11$_{17-43}$-HLA-A*02:01 SC X-ray crystal structure, and (F) the 9-mer peptide from HLA-A*02:01 refolded with the peptide T^{27}LFDEPPPL^{32}. All maps are shown as blue mesh and contoured at 1 σ.

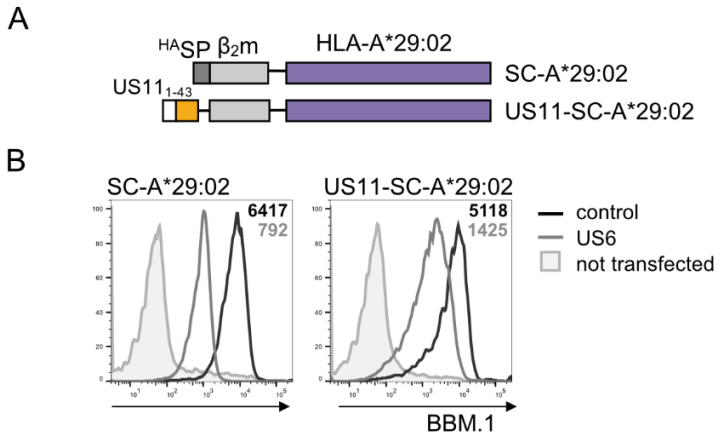

Fig S5. **Optimal US11 LCR targeting of HLA-A*29:02 and A*68:02 is tapasin-dependent.**
(A) Schematic representation of HLA-A*29:02 single-chain (SC) constructs. ^{HA}SP, signal peptide of haemagglutinin. (B) HLA-A*29:02 SC constructs encoded in pcDNA3.1 were transiently co-transfected with pIRES-EGFP encoding a control protein or US6 into β_2m-deficient FO-1 cells. At 20 h post-transfection SC-A29:02 and US11-SC-A*29:02 cell surface expression was analyzed by flow cytometry using the anti-β_2m mAb BBM.1. Representative histograms are shown.

A

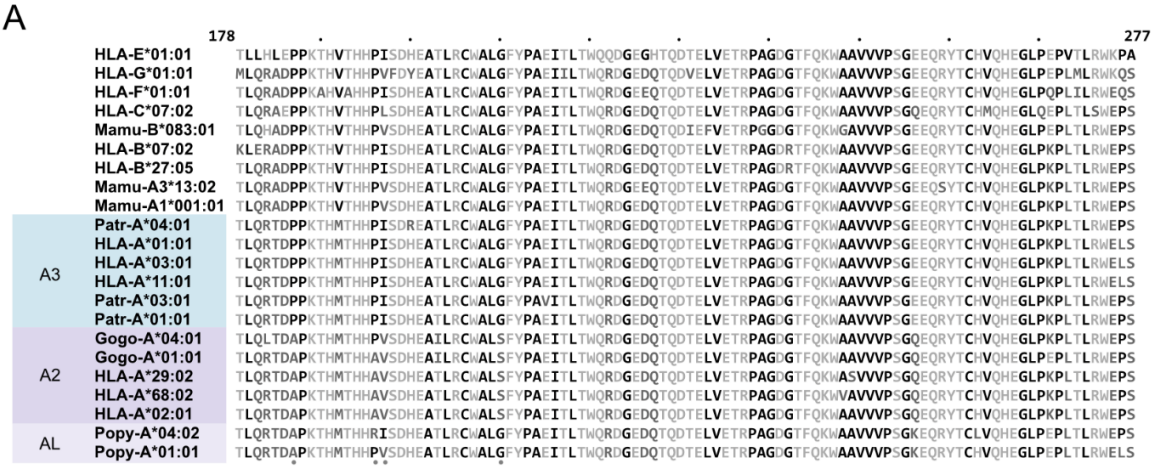
178
277
HLA-E*01:01 TLLHLEPPKTHVTHHPISDHEATLRCWALGFYPAEITLTWQQDGEGHTQDTELVETRPAGDGTFQKWAAVVVPSGEEQRYTCHVQHEGLPEPVTLRWKPA
HLA-G*01:01 MLQRADPPKTHVTHHPVFDYEATLRCWALGFYPAEIILTWQRDGEDQTQDVELVETRPAGDGTFQKWAAVVVPSGEEQRYTCHVQHEGLPEPLMLRWKQS
HLA-F*01:01 TLQRADPPKAHVAHHPISDHEATLRCWALGFYPAEITLTWQRDGEEQTQDTELVETRPAGDGTFQKWAAVVVPSGEEQRYTCHVQHEGLPQPLILRWEQS
HLA-C*07:02 TLQRAEPPKTHVTHHPLSDHEATLRCWALGFYPAEITLTWQRDGEDQTQDTELVETRPAGDGTFQKWAAVVVPSGQEQRYTCHMQHEGLQEPLTLSWEPS
Mamu-B*083:01 TLQHADPPKTHVTHHPVSDHEATLRCWALGFYPAEITLTWQRDGEDQTQDIEFVETRPGGDGTFQKWGAVVVPSGEEQRYTCHVQHEGLPEPLTLRWEPS
HLA-B*07:02 KLERADPPKTHVTHHPISDHEATLRCWALGFYPAEITLTWQRDGEDQTQDTELVETRPAGDRTFQKWAAVVVPSGEEQRYTCHVQHEGLPKPLTLRWEPS
HLA-B*27:05 TLQRADPPKTHVTHHPISDHEATLRCWALGFYPAEITLTWQRDGEDQTQDTELVETRPAGDRTFQKWAAVVVPSGEEQRYTCHVQHEGLPKPLTLRWEPS
Mamu-A3*13:02 TLQRADPPKTHVTHHPVSDHEATLRCWALGFYPAEITLTWQRDGEEQTQDTELVETRPAGDGTFQKWAAVVVPSGEEQSYTCHVQHEGLPKPLTLRWEPS
Mamu-A1*001:01 TLQRADPPKTHVTHHPVSDHEATLRCWALGFYPAEITLTWQRDGEDQTQDTELVETRPAGDGTFQKWAAVVVPSGEEQRYTCHVQHEGLPKPLTLRWEPS
A3 Patr-A*04:01 TLQRTDPPKTHMTHHPISDREATLRCWALGFYPAEITLTWQRDGEDQTQDTELVETRPAGDGTFQKWAAVVVPSGEEQRYTCHVQHEGLPKPLTLRWEPS
A3 HLA-A*01:01 TLQRTDPPKTHMTHHPISDHEATLRCWALGFYPAEITLTWQRDGEDQTQDTELVETRPAGDGTFQKWAAVVVPSGEEQRYTCHVQHEGLPKPLTLRWELS
A3 HLA-A*03:01 TLQRTDPPKTHMTHHPISDHEATLRCWALGFYPAEITLTWQRDGEDQTQDTELVETRPAGDGTFQKWAAVVVPSGEEQRYTCHVQHEGLPKPLTLRWELS
A3 HLA-A*11:01 TLQRTDPPKTHMTHHPISDHEATLRCWALGFYPAEITLTWQRDGEDQTQDTELVETRPAGDGTFQKWAAVVVPSGEEQRYTCHVQHEGLPKPLTLRWELS
A3 Patr-A*03:01 TLQRTDPPKTHMTHHPISDHEATLRCWALGFYPAVITLTWQRDGEDQTQDTELVETRPAGDGTFQKWAAVVVPSGEEQRYTCHVQHEGLPKPLTLRWEPS
A3 Patr-A*01:01 TLQRTDPPKTHMTHHPISDHEATLRCWALGFYPAEITLTWQRDGEDQTQDTELVETRPAGDGTFQKWAAVVVPSGEEQRYTCHVQHEGLPKPLTLRWEPS
A2 Gogo-A*04:01 TLQLTDAPKTHMTHHPVSDHEAILRCWALSFYPAEITLTWQRDGEDQTQDTELVETRPAGDGTFQKWAAVVVPSGQEQRYTCHVQHEGLPKPLTLRWEPS
A2 Gogo-A*01:01 TLQRTDAPKTHMTHHAVSDHEAILRCWALSFYPAEITLTWQRDGEDQTQDTELVETRPAGDGTFQKWAAVVVPSGQEQRYTCHVQHEGLPEPLTLRWEPS
A2 HLA-A*29:02 TLQRTDAPKTHMTHHAVSDHEATLRCWALSFYPAEITLTWQRDGEDQTQDTELVETRPAGDGTFQKWASVVVPSGQEQRYTCHVQHEGLPKPLTLRWEPS
A2 HLA-A*68:02 TLQRTDAPKTHMTHHAVSDHEATLRCWALSFYPAEITLTWQRDGEDQTQDTELVETRPAGDGTFQKWVAVVVPSGQEQRYTCHVQHEGLPKPLTLRWEPS
A2 HLA-A*02:01 TLQRTDAPKTHMTHHAVSDHEATLRCWALSFYPAEITLTWQRDGEDQTQDTELVETRPAGDGTFQKWAAVVVPSGQEQRYTCHVQHEGLPKPLTLRWEPS
AL Popy-A*04:02 TLQRTDAPKTHMTHHRISDHEATLRCWALGFYPAEITLTWQRDGEDQTQDTELVETRPAGDGTFQKWAAVVVPSGKEQRYTCLVQHEGLPEPLTLRWEPS
AL Popy-A*01:01 TLQRTDAPKTHMTHHPVSDHEATLRCWALGFYPAEITLTWQRDGEDQTQDTELVETRPAGDGTFQKWAAVVVPSGKEQRYTCHVQHEGLPEPLTLRWELS

B

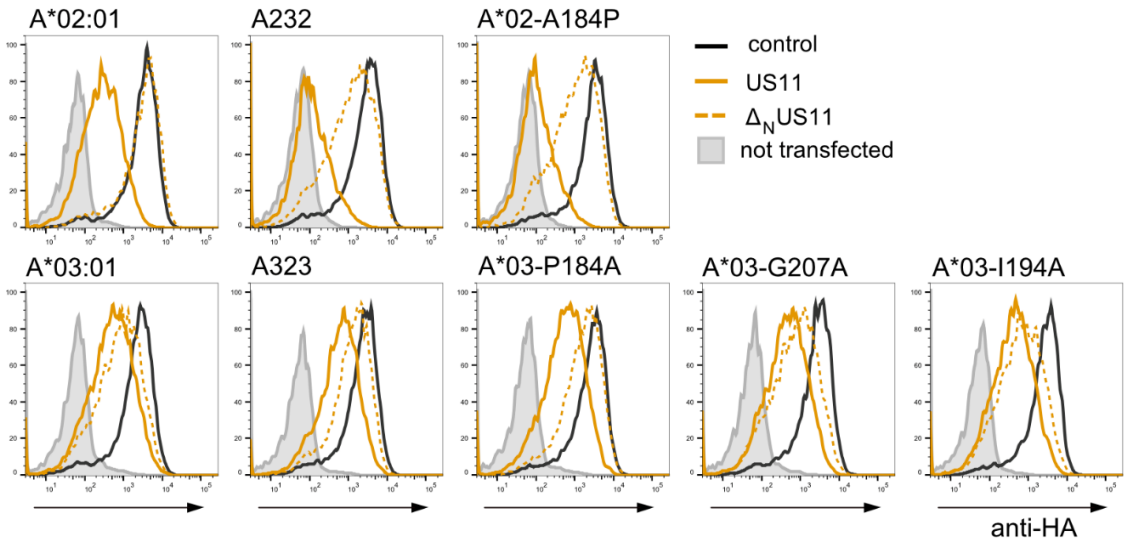
A*02:01
A232
A*02-A184P
control
US11
Δ_NUS11
not transfected
A*03:01
A323
A*03-P184A
A*03-G207A
A*03-I194A
anti-HA

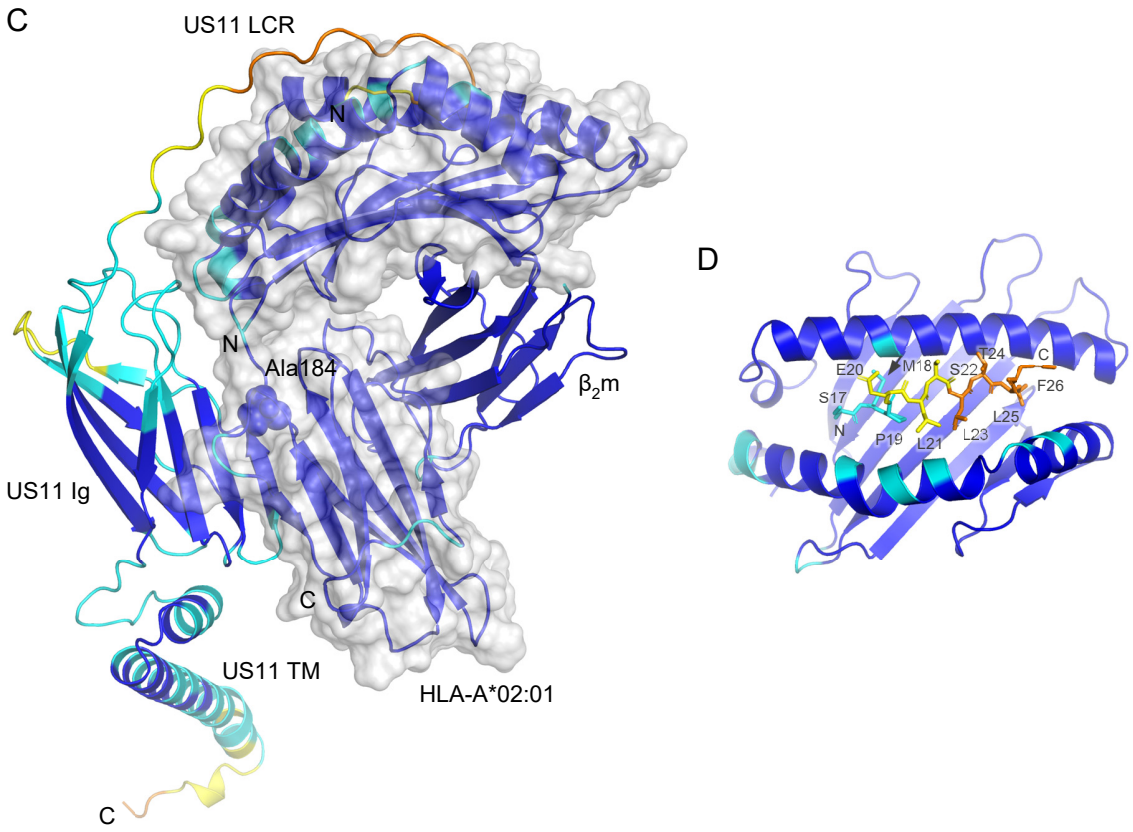

Fig S6. A single residue in the α3 domain dictates N-terminus-independent regulation of HLA-A by US11. (A) Muscle alignment [13] of the α3 domain residues 178-277 of a few representative human and primate MHC-I molecules. Labeled residues from Fig 6A are marked with a grey dot. (B) HeLa cells were transiently co-transfected with plasmids encoding HA-tagged HLA-A and pIRES-EGFP encoding US11, Δ_NUS11, or a control protein. At 20 h post-transfection HLA-I surface expression was determined by flow cytometry (anti-HA) on EGFP-positive cells. Representative histograms are shown. (C) Cartoon representation of the AlphaFold-Multimer prediction of the full-length US11/HLA-A*02:01 complex coloured based on the per-residue confidence score (pLDDT): Dark-blue = very-high confidence (pLDDT > 90), Light-blue = confident (90 > pLDDT > 70), Yellow = low confidence (70 > pLDDT > 50), Orange = very low confidence (pLDDT < 50). Surface representation of HLA-A*02:01 heavy chain is displayed for reference, and Ala184 is highlighted as spheres. (D) Close-up of the peptide-binding groove of (C) with US11 LCR residues indicated in single letter code.

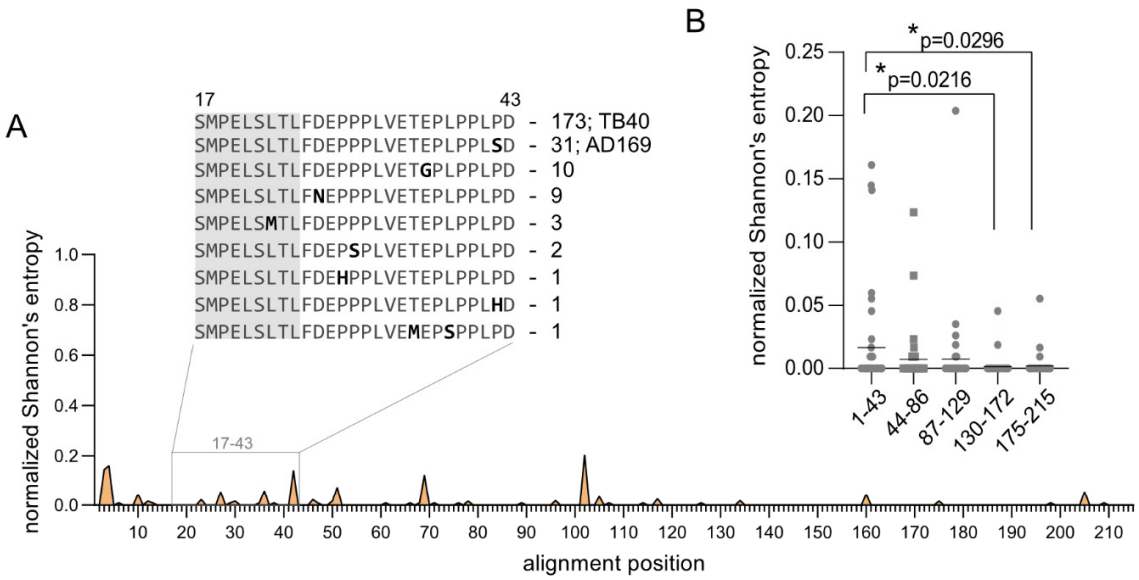

C

	saS3	saS13	saS33	aoA28	aoA29	ceUS11	rhUS11	cUS11	hUS11	hUS9	hUS10
saS3	100.00	15.84	19.17	18.80	19.09	21.78	16.44	17.54	20.49	16.59	14.38
saS13	15.84	100.00	24.35	28.09	26.62	18.75	17.35	19.07	15.26	17.65	16.77
saS33	19.17	24.35	100.00	27.36	23.16	15.94	18.31	15.27	17.00	14.75	17.37
aoA28	18.80	28.09	27.36	100.00	47.85	17.51	17.94	17.70	14.43	17.04	21.97
aoA29	19.09	26.62	23.16	47.85	100.00	19.81	19.27	15.76	17.26	18.43	16.15
ceUS11	21.78	18.75	15.94	17.51	19.81	100.00	30.91	29.33	32.34	20.19	13.42
rhUS11	16.44	17.35	18.31	17.94	19.27	30.91	100.00	26.83	24.75	20.47	16.67
cUS11	17.54	19.07	15.27	17.70	15.76	29.33	26.83	100.00	45.45	29.52	13.48
hUS11	20.49	15.26	17.00	14.43	17.26	32.34	24.75	45.45	100.00	28.29	12.95
hUS9	16.59	17.65	14.75	17.04	18.43	20.19	20.47	29.52	28.29	100.00	14.57
hUS10	14.38	16.77	17.37	21.97	16.15	13.42	16.67	13.48	12.95	14.57	100.00
CMV in	New World Monkeys					Old World Monkeys		Great Apes			

Fig S7. US11 evolved an LCR-dependent strategy specifically to counteract A2 lineage escape from N-terminus-independent antagonism. (A) Diagram shows the normalized Shannon's entropy of 231 US11 HCMV sequences [14]. Each US11 alignment position was calculated in python3 using biopython [15], numpy [16] and scipy [17]. In the N-terminal region (positions 17-43), 173 sequences were identical to the TB40 strain US11 (top sequence) and 31 sequences were identical to the AD169 US11. All variants are shown; variable residues are highlighted in bold letters and the number of identified sequences are shown to the right. The HLA-A*02 peptide mimic is colored in grey. (B) The multiple sequence alignment from (A) was split into 5 equally large regions, for each region entropies per position and mean entropy was plotted. Significance was calculated with an one-way ANOVA using Dunnett's multiple comparison test. Only significant difference to positions 1-43 are shown. (C) Percent sequence identity of primate cytomegalovirus encoded US proteins most closely related to HCMV US11 (BLASTP). HCMV US9 and US10 were included as comparison for non-US11 proteins in the US6 protein family. Sequence

identity was determined by Muscle sequence alignment [13] of the following sequences: *human betaherpesvirus 5* (strain AD169): US9, US10, US11; *panine betaherpesvirus 2*: US11, (NP_612784.1); *rhesus cytomegalovirus strain 68-1*: Rh189 (QQL10478.1); *cercopithecine betaherpesvirus 5*: US11 (AEV80690.1); *saimiriine betaherpesvirus*: S3 (YP_004940179.1), S13 (YP_004940292.1), S33 (YP_004940317.1); *aotine betaherpesvirus 1*: A29, (YP_004940154.1), A28 (YP_004940153.1). The orange box marks US11 homologs and the grey box marks US6 protein family members in CMVs of New World Monkeys.

S1 Table. Data collection and refinement statistics.

Data collection statistics	***US11-SC***	***HLA-A*02:01^{TLF}***
X-ray source	MX2 Australian Synchrotron	MX2 Australian Synchrotron
Spacegroup	*P* 2_1	*P* 2_1 2_1 2_1
Cell dimensions		
a, b, c (Å)	52.39, 80.50, 56.08	59.87, 79.27, 110.66
α, β, γ (°)	89.92, 113.49, 90.19	90, 90, 90
Resolution (Å)	48.04 - 1.80 (1.84 – 1.80)	40.64 - 1.60 (1.66 - 1.60)
Total number of observations	139,869 (8,382)	689,942 (33,792)
No. unique observations	39,611 (2,325)	70,264 (3,437)
Multiplicity	3.5 (3.6)	9.8 (9.8)
Data completeness (%)	99.90 (99.9)	100 (100)
I/σ_I	6.8 (1.2)	6.1 (1.5)
R_{pim} (%)	8.1 (84.2)	8.6 (59.4)
CC (1/2)	0.996 (0.704)	0.990 (0.626)
Refinement statistics		
No. atoms		
Macromolecules	3131	3162
Ligands	28	23
Water	239	472
$^1R_{factor}$ (%)	20.61 (36.97)	18.01 (25.40)
R_{free} (%)	23.89 (45.22)	20.31 (28.53)
root mean squared deviation from ideality		
Bond lengths (Å)	0.006	0.007
Bond angles (°)	1.13	1.19
Ramachandran plot		
Favoured regions (%)	98.95	98.68
Allowed regions (%)	1.05	1.32
Disallowed regions (%)	0	0
B factor, all atoms (Å^2)	34.73	27.93

Statistics for the highest-resolution shell are shown in parentheses.

SI References

1 Zimmermann, C., Kowalewski, D., Bauersfeld, L., Hildenbrand, A., Gerke, C., Schwarzmuller, M., Le-Trilling, V. T. K., Stevanovic, S., Hengel, H., Momburg, F. and Halenius, A., HLA-B locus products resist degradation by the human cytomegalovirus immunoevasin US11. *PLoS Pathog* 2019. 15: e1008040.

2 Rolle, A., Meyer, M., Calderazzo, S., Jager, D. and Momburg, F., Distinct HLA-E Peptide Complexes Modify Antibody-Driven Effector Functions of Adaptive NK Cells. *Cell Rep* 2018. 24: 1967-1976 e1964.

3 Lubke, M., Spalt, S., Kowalewski, D. J., Zimmermann, C., Bauersfeld, L., Nelde, A., Bichmann, L., Marcu, A., Peper, J. K., Kohlbacher, O., Walz, J. S., Le-Trilling, V. T. K., Hengel, H., Rammensee, H. G., Stevanovic, S. and Halenius, A., Identification of HCMV-derived T cell epitopes in seropositive individuals through viral deletion models. *J Exp Med* 2020. 217.

4 Jurtz, V., Paul, S., Andreatta, M., Marcatili, P., Peters, B. and Nielsen, M., NetMHCpan-4.0: Improved Peptide-MHC Class I Interaction Predictions Integrating Eluted Ligand and Peptide Binding Affinity Data. *J Immunol* 2017. 199: 3360-3368.

5 Riedl, A., Gruber, S. and Ruzsics, Z., Novel conditional plasmids regulated by chemical switches provide versatile tools for genetic engineering in Escherichia coli. *Plasmid* 2020. 111: 102531.

6 Le, V. T., Trilling, M. and Hengel, H., The cytomegaloviral protein pUL138 acts as potentiator of tumor necrosis factor (TNF) receptor 1 surface density to enhance ULb'-encoded modulation of TNF-alpha signaling. *J Virol* 2011. 85: 13260-13270.

7 Le-Trilling, V. T. K., Becker, T., Nachshon, A., Stern-Ginossar, N., Scholer, L., Voigt, S., Hengel, H. and Trilling, M., The Human Cytomegalovirus pUL145 Isoforms Act as Viral DDB1-Cullin-Associated Factors to Instruct Host Protein Degradation to Impede Innate Immunity. *Cell Rep* 2020. 30: 2248-2260 e2245.

8 Stam, N. J., Vroom, T. M., Peters, P. J., Pastoors, E. B. and Ploegh, H. L., HLA-A- and HLA-B-specific monoclonal antibodies reactive with free heavy chains in western blots, in formalin-fixed, paraffin-embedded tissue sections and in cryo-immuno-electron microscopy. *Int Immunol* 1990. 2: 113-125.

9 Brodsky, F. M., Parham, P., Barnstable, C. J., Crumpton, M. J. and Bodmer, W. F., Monoclonal antibodies for analysis of the HLA system. *Immunol Rev* 1979. 47: 3-61.

10 Brodsky, F. M., Bodmer, W. F. and Parham, P., Characterization of a monoclonal anti-beta 2-microglobulin antibody and its use in the genetic and biochemical analysis of major histocompatibility antigens. *Eur J Immunol* 1979. 9: 536-545.

11 Gewurz, B. E., Gaudet, R., Tortorella, D., Wang, E. W., Ploegh, H. L. and Wiley, D. C., Antigen presentation subverted: Structure of the human cytomegalovirus protein US2 bound to the class I molecule HLA-A2. *Proc Natl Acad Sci U S A* 2001. 98: 6794-6799.

12 Jarnot, P., Ziemska-Legiecka, J., Dobson, L., Merski, M., Mier, P., Andrade-Navarro, M. A., Hancock, J. M., Dosztanyi, Z., Paladin, L., Necci, M., Piovesan, D., Tosatto, S. C. E., Promponas, V. J., Grynberg, M. and Gruca, A., PlaToLoCo: the first web meta-server for visualization and annotation of low complexity regions in proteins. *Nucleic Acids Res* 2020. 48: W77-W84.

13 Madeira, F., Pearce, M., Tivey, A. R. N., Basutkar, P., Lee, J., Edbali, O., Madhusoodanan, N., Kolesnikov, A. and Lopez, R., Search and sequence analysis tools services from EMBL-EBI in 2022. *Nucleic Acids Res* 2022.

14 Charles, O. J., Venturini, C., Gantt, S., Atkinson, C., Griffiths, P., Goldstein, R. A. and Breuer, J., Genomic and geographical structure of human cytomegalovirus. *Proc Natl Acad Sci U S A* 2023. 120: e2221797120.

15 Cock, P. J., Antao, T., Chang, J. T., Chapman, B. A., Cox, C. J., Dalke, A., Friedberg, I., Hamelryck, T., Kauff, F., Wilczynski, B. and de Hoon, M. J., Biopython: freely available Python tools for computational molecular biology and bioinformatics. *Bioinformatics* 2009. 25: 1422-1423.

16 Harris, C. R., Millman, K. J., van der Walt, S. J., Gommers, R., Virtanen, P., Cournapeau, D., Wieser, E., Taylor, J., Berg, S., Smith, N. J., Kern, R., Picus, M., Hoyer, S., van Kerkwijk, M. H., Brett, M., Haldane, A., Del Rio, J. F., Wiebe, M., Peterson, P., Gerard-Marchant, P., Sheppard, K., Reddy, T., Weckesser, W., Abbasi, H., Gohlke, C. and Oliphant, T. E., Array programming with NumPy. *Nature* 2020. 585: 357-362.

17 Virtanen, P., Gommers, R., Oliphant, T. E., Haberland, M., Reddy, T., Cournapeau, D., Burovski, E., Peterson, P., Weckesser, W., Bright, J., van der Walt, S. J., Brett, M., Wilson, J., Millman, K. J., Mayorov, N., Nelson, A. R. J., Jones, E., Kern, R., Larson, E., Carey, C. J., Polat, I., Feng, Y., Moore, E. W., VanderPlas, J., Laxalde, D., Perktold, J., Cimrman, R., Henriksen, I., Quintero, E. A., Harris, C. R., Archibald, A. M., Ribeiro, A. H., Pedregosa, F., van Mulbregt, P. and SciPy, C., SciPy 1.0: fundamental algorithms for scientific computing in Python. *Nat Methods* 2020. 17: 261-272.